해부 · 생물인류학 제 38 권 제 4 호
Anat Biol Anthropol Vol. 38, No. 4 (2025) pp. 291~302
https://doi.org/10.11637/aba.2025.38.4.291

Original Article

Effect of Cooling Temperature on Shrinkage and Pressure-Induced Discomfort in Thermoplastic Head and Neck Immobilization Masks for Radiotherapy

Yun Sung Shin[1], Young Min Kim[1], So Hyun Park[1], Myeongsoo Kim[1]

Department of Radiation Oncology, Keimyung University Dongsan Hospital

Abstract : Thermoplastic head-and-neck immobilization masks improve setup reproducibility in radiation therapy but may undergo shrinkage and generate local pressure, affecting geometric stability and patient comfort. This study investigated how residual temperature after molding influences long-term shape stability and contact pressure of thermoplastic masks. Two commercially available mask systems (manufacturers A and B) were molded on a RANDO anthropomorphic phantom under three cooling conditions (16°C, 26°C, 36°C). Computed tomography scans were acquired immediately, and at 7 and 30 days, and mask geometries were compared with the initial shape using the Dice similarity coefficient (DICE). Local contact pressure at the forehead, nasal bridge, neck, chest, and shoulder was measured using pressure-sensitive film and converted to pressure (MPa). For both manufacturers, masks molded at 16°C showed the highest DICE values, whereas 36°C yielded the lowest, indicating greater shrinkage and reduced geometric stability at higher residual temperatures. DICE values decreased slightly over 30 days, with the largest decline at 36°C. For manufacturer A, pressure did not change significantly with temperature ($p=0.1155$). For manufacturer B, pressure increased and became more variable at 36°C, especially at the nasal bridge and neck ($p=0.0483$). Residual temperature after molding is therefore a critical parameter. Cooling masks to lower temperatures and considering material thermal sensitivity may help maintain geometric stability and reduce patient-perceived pressure.

Keywords : Thermoplastic mask, Head and neck radiotherapy, Cooling temperature, Mask shrinkage

INTRODUCTION

The precision of radiation therapy is directly linked to patient setup reproducibility, which is essential for maintaining consistency of the planned dose distribution and ensuring treatment accuracy. In particular, the head and neck (HN) region has a highly complex anatomy, and radiation-sensitive organs such as the spinal cord, salivary glands, larynx, and oral mucosa are located in close proximity to the tumor. As a result, it is difficult to secure a sufficient safety margin around the target volume. In other words, expansion of the planning target volume (PTV)

The author(s) agree to abide by the good publication practice guideline for medical journals.
The author(s) declare that there are no conflicts of interest.
Received: November 26, 2025; **Revised:** December 19, 2025; **Accepted:** December 22, 2025
Correspondence to: Myeongsoo Kim (Department of Radiation Oncology, Keimyung University Dongsan Hospital, Daegu 42601, Republic of Korea)
E-mail: mskim@dsmc.or.kr

ISSN 2671-566X (Online)

to compensate for positioning and motion uncertainties during treatment is limited, and even submillimeter- to millimeter-scale setup errors may lead to clinically relevant underdose to the target or overdose to adjacent normal tissues [1]. Owing to these clinical characteristics, precise immobilization systems have become a key component of high-precision radiation therapy techniques such as intensity-modulated radiation therapy (IMRT), volumetric modulated arc therapy (VMAT), stereotactic radiosurgery (SRS), and stereotactic body radiotherapy (SBRT). Among these, thermoplastic head-and-neck immobilization masks are widely regarded as the standard fixation device because they provide excellent conformity to patient anatomy and high setup reproducibility [2].

Several studies have quantitatively evaluated the setup reproducibility of thermoplastic masks. Gilbeau et al. divided 30 patients with brain and head-and-neck tumors into three immobilization groups using thermoplastic masks with three-point, four-point, or five-point fixation, and acquired weekly orthogonal portal images during treatment. By comparing two-dimensional and three-dimensional coordinates between these portal images and the simulation films, they analyzed setup errors. They reported that, in the head and neck region, the standard deviation of the total displacement was approximately 2.2 mm, and 90% of the three-dimensional displacement vectors remained below 4.5 mm, indicating that thermoplastic mask-based immobilization provides clinically acceptable translational setup accuracy [3].

Boda-Heggemann et al. evaluated the repositioning accuracy of two different mask systems using true three-dimensional/three-dimensional (3D/3D) image registration with cone-beam computed tomography (CBCT). After image-guided corrections before treatment, the residual setup errors and intrafractional motion were quantified, and the three-dimensional displacement vectors were reported to remain within approximately 1~2 mm. These findings demonstrate that, when combined with image-guided radiation therapy (IGRT), thermoplastic mask immobilization can achieve the level of accuracy required for high-precision radiation therapy [4].

However, despite this excellent setup accuracy and structural stability, the use of thermoplastic masks has been associated with psychological anxiety, claustrophobia, and pressure-related discomfort, and these symptoms are not limited to subjective nuisance alone but may act as clinically relevant barriers to treatment. Nixon et al. conducted a mixed-methods study in patients undergoing head-and-neck radiotherapy using a modified Distress Thermometer and reported that approximately 26% of patients experienced mask-related anxiety or distress [5]. In a subsequent prospective study, they repeatedly assessed distress levels during the treatment course and showed that, in a subset of patients, mask-related anxiety can persist or even worsen over time [6].

In addition, a scoping review by Lastrucci et al. summarized evidence that closed-face thermoplastic masks may provoke discomfort and claustrophobia, which can negatively affect patient experience, psychological adherence, and intrafractional stability by increasing treatment-related movement [7]. Such deterioration in patient experience may ultimately lead to increased motion during irradiation, treatment avoidance behaviors, and reduced compliance, thereby negatively impacting both treatment efficiency and clinical outcomes.

To address these issues, open-face thermoplastic masks have recently been introduced as an alternative to conventional full-face designs, with several reports suggesting that they can alleviate claustrophobia and breathing discomfort while maintaining adequate setup reproducibility. Nevertheless, open-face masks are still manufactured through the same sequence of heating, molding, and cooling, and the resulting material shrinkage and long-term residual thermal deformation cannot be fully avoided. Therefore, increasing the degree of facial exposure alone is unlikely to provide a complete solution for improving patient experience; a complementary approach that considers the thermal stability of the mask material and optimizes the manufacturing and cooling process from a physical and procedural standpoint remains necessary.

Dovell et al. reported that the degree of post-fabrication shrinkage of thermoplastic masks differs depending on the mask material, and that greater shrinkage is associated with reduced comfort during wear [8,9]. These findings suggest that the thermal handling conditions applied to thermoplastic masks can influence both the pressure exerted on the patient and the long-term structural stability of the mask. However, previous studies have mainly focused on comparing different materials, and there is a relative lack of research that quantitatively links the cooling temperature immediately after molding (thermal residual condition) to subsequent changes in structural stability and contact pres-

Fig. 1. Workflow for softening and molding thermoplastic head-and-neck immobilization masks using an air oven.

sure during mask use.

Therefore, in the present study, we fabricated thermoplastic masks under anthropomorphic phantom-based conditions and quantitatively evaluated time-dependent changes in mask geometry and contact pressure as a function of cooling temperature and residual heat immediately after molding. The findings of this study are expected to contribute to the clinical standardization of thermoplastic mask manufacturing processes and to the development of strategies aimed at improving patient experience during high-precision radiation therapy.

MATERIALS AND METHODS

1. Fabrication of thermoplastic head-and-neck masks

In this study, two types of commercially available thermoplastic head-and-neck mask sheets were selected, and three sheets of each type (six sheets in total) were used for the experiments. To simulate in vivo conditions, a RANDO anthropomorphic phantom (The Phantom Laboratory, USA) was used as the standard human phantom [10,11]. To mimic the mechanical properties of human skin at the mask-surface interface, the phantom surface was uniformly coated with a silicone material originally designed for fabrication of three-dimensional (3D) radiotherapy boluses [12]. Silicone-based phantoms and boluses are widely used in radiotherapy because their mechanical behavior and radiation attenuation properties closely approximate those of human soft tissue [13,14].

Each thermoplastic sheet was placed in an air oven and uniformly softened by heating at 73°C for 5 minutes, and then molded to conform closely to the head, neck, and upper chest of the anthropomorphic phantom (Fig. 1). During molding, the sheet was carefully pressed so that it fully adhered to the phantom surface, and no additional external pressure was applied other than the locking mechanism of the mask fixation frame, in order to minimize unintended mechanical interference.

Immediately after molding, the mask was kept fixed on the phantom, and the assigned cooling procedure was initiated. Two cooling methods were used: air cooling with a handheld fan and cold cooling using ice packs. The overall molding workflow—heating, molding, and cooling—was designed to reproduce routine clinical practice, and the same standardized procedure was applied to all thermoplastic sheets.

Given the standardized manufacturing process of commercial thermoplastic masks, the study design utilized one sheet per condition to evaluate physical phase-change behaviors, proceeding on the premise that inter-sample variability in material properties is minimal compared to the distinct effects of temperature.

2. Temperature measurement and measurement sites

For quantitative assessment of the cooling process, five anatomical sites on the anthropomorphic phantom—forehead, nasal bridge, neck, shoulder, and chest—were se-

Fig. 2. Locations of temperature measurement points on the thermoplastic head-and-neck mask and example of surface temperature measurement on the anthropomorphic head-and-shoulder phantom.

lected as temperature measurement points. These regions correspond to the main contact areas of head-and-neck thermoplastic masks and were chosen based on previous reports that the design of the forehead and anterior facial opening strongly influences immobilization performance, and that head-and-shoulder-type masks extending over the shoulders and lower neck can reduce setup errors [4,15].

Surface temperatures at each site were measured using a non-contact infrared thermometer (FS-300, HUBDIC, Republic of Korea; measurement range 0~100°C, resolution 0.1°C, operating temperature 16~40°C, relative humidity ≤95%). Measurements were performed every 5 seconds from immediately after heating until completion of the cooling phase. At each time point, three consecutive readings were acquired at each site, and their average was used for analysis. The end of cooling for a given condition was defined as the time point at which the measured temperature at each site reached the predefined target value (16°C, 26°C, or 36°C; Fig. 2). These three target temperatures were specifically selected to simulate distinct clinical scenarios. The 36°C condition represents a scenario of "insufficient cooling," where the mask is considered set while still near the patient's body temperature, potentially leading to inadequate hardening. The 26°C condition corresponds to standard passive air cooling within a typical treatment room environment. Finally, the 16°C condition simulates an "active cooling" protocol, achievable through methods such as cold packs or forced air, aimed at ensuring rapid and complete thermal stabilization. The measurement uncertainty and repeatability of the thermometer were verified by initial calibration before the experiment.

Fig. 3. CT acquisition setup for three-dimensional evaluation of thermoplastic head-and-neck mask deformation after molding.

3. Image analysis for CT scans

To quantitatively evaluate time-dependent shrinkage and torsional deformation of the thermoplastic masks after molding, computed tomography (CT) images were acquired using a SOMATOM Definition AS scanner (Siemens Healthineers, Germany) (Fig. 3). The acquisition parameters were as follows: tube voltage 120 kVp, pitch 0.85, and slice thickness 2 mm. Automatic exposure control (AEC) was applied to reduce image noise.

The field of view (FOV) was adjusted to include the entire mask and the base plate of the immobilization system. For all scans, the phantom was repositioned in the same setup with identical head, neck, and shoulder alignment to ensure reproducible geometry across all measurement time points.

The acquired images were stored in Digital Imaging and Communications in Medicine (DICOM) format and imported into a commercial image processing platform (MIM Software Inc., Cleveland, OH, USA) for three-dimensional (3D) image reconstruction (Fig. 4). CT datasets obtained at each time point (immediately after molding, 7 days, and 30 days) were then co-registered using image registration, and subsequent analyses were performed to calculate surface displacement and volume change of the thermoplastic masks

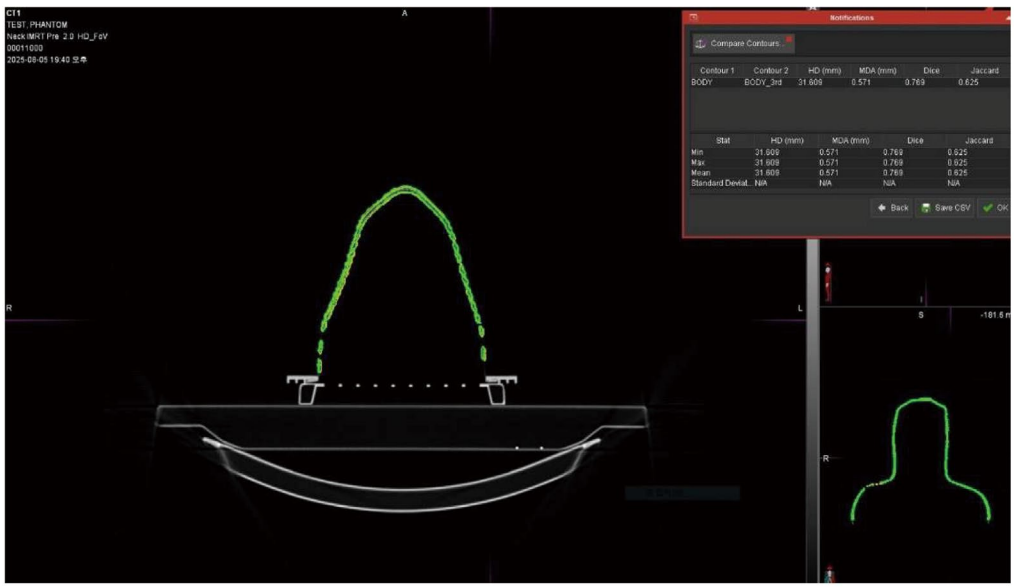

Fig. 4. Example of Dice similarity coefficient (DICE) analysis of thermoplastic mask contours using MIM software.

over time. Through this process, the time-dependent deformation behavior and structural stability of the thermoplastic masks after fabrication were quantitatively evaluated.

The geometric information of the thermoplastic masks was analyzed using MIM Software (MIM Software Inc., USA) to compare shape changes according to cooling temperature (16°C, 26°C, and 36°C) and imaging time point. To quantitatively assess shape similarity, the Dice similarity coefficient (DICE) was used [10,16]. DICE is a statistical index that represents the degree of overlap between two regions. For two sets A and B, it is defined as:

$$DICE = 2|A \cap B| / (|A| + |B|) \quad \text{(Eq. 1)}$$

The DICE value ranges from 0 to 1; values closer to 1 indicate a higher degree of overlap and thus better geometric agreement between the two regions, whereas values closer to 0 indicate minimal overlap.

4. Analysis of pressure-sensitive film

To quantitatively assess the local contact pressure that would be perceived by a patient, an ink-type pressure-sensitive film (PSF) was used. This dry-type PSF changes the color density of an indicator layer when pressure is applied, allowing the applied pressure to be estimated from the resulting color intensity. In this study, we used a 4LW-type PSF with the lowest available measurement range provided by the manufacturer (0.02~0.30 megapascal [MPa], equivalent to 0.203~3.059 kg/cm^2). For each measurement condition, pressure readings were acquired five times and the results were subjected to statistical analysis. The pressure measurement sites were defined as the forehead, nasal bridge, neck, shoulder, and chest of the anthropomorphic phantom (Fig. 5). At each site, the thermoplastic mask was positioned and fixed in the treatment configuration, and the resulting local contact pressure was recorded using the pressure-sensitive film after 11 seconds of continuous loading. All measurements were performed under identical conditions (same phantom position and same mask fixation method) to ensure reproducibility of repeated measurements.

For each anatomical site, the RGB (red, green, blue) values obtained from the pressure-sensitive film after 11 seconds were converted to pressure values using the calibration table provided by the film manufacturer. The contact pressure exerted by the thermoplastic mask was quantified based on the change in RGB intensity, and the measured RGB values were finally converted to pressure in megapascals (MPa) using the following linear regression equation:

$$MPa = -0.120 \times RGB + 30.6 \quad \text{(Eq. 2)}$$

The developed color layer of the pressure-sensitive film was digitized using a flatbed scanner from the Epson Expression series (Expression 13000XL; Seiko Epson

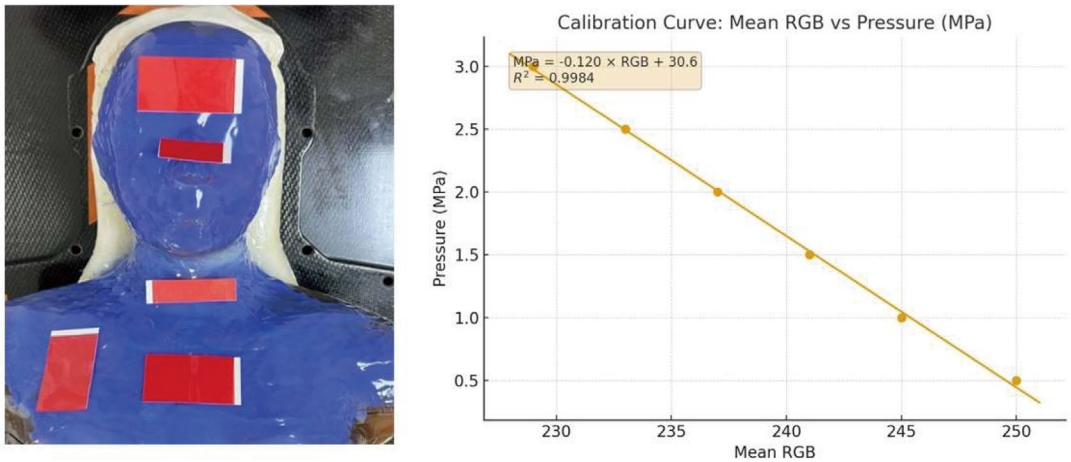

Fig. 5. Placement of pressure-sensitive film at anatomical contact sites and manufacturer-provided calibration curve for converting RGB values to contact pressure.

Fig. 6. Extraction of red channel intensity (RGB) from scanned pressure-sensitive film using ImageJ for quantitative pressure analysis.

Corp., Japan) at a resolution of 1000 dots per inch (dpi). According to the manufacturer's specifications, the Expression 13000XL supports an optical resolution of up to 2400 × 4800 dpi; therefore, scanning at 1000 dpi was well within the optical performance range of the device.

The scanned pressure-sensitive films were quantitatively analyzed based on pixel-wise color information in the RGB color model. For each film, the median value of the red (R) channel within a predefined region of interest (ROI) was used as the representative metric of ink density. The median R value, defined as the middle value of all pixel intensities within the ROI, is less sensitive to outliers and is therefore suitable for evaluating the density of the transferred ink. Pixel values were extracted using ImageJ (National Institutes of Health, version 1.54p), an open-source image analysis software package (Fig. 6) [17,18]. For each film, five ROIs of 300 × 300 pixels were sampled within the developed area, and the mean of the median R values from these five ROIs was used for subsequent analysis.

The converted pressure data were organized by mask manufacturer (A and B), cooling temperature condition (16°C, 26°C, and 36°C), and anatomical site (forehead, nasal bridge, neck, chest, and shoulder). Before performing any inferential statistical analyses, the assumptions of nor-

mality and homogeneity of variance were evaluated using the Shapiro-Wilk test and Levene's test, respectively.

For each manufacturer, a two-way analysis of variance (two-way ANOVA) was conducted to determine whether cooling temperature had a statistically significant effect on contact pressure. In this analysis, temperature (Temp) and anatomical site (Part) were treated as independent variables, and pressure (Pressure) was used as the dependent variable. The primary objective was to examine whether, after accounting for pressure differences between anatomical sites (i.e., site-related variability and noise), the temperature factor alone exerted a statistically significant influence on pressure values ($p < 0.05$).

When the temperature factor showed a statistically significant effect, Tukey's honestly significant difference (HSD) post hoc test was performed to identify which specific temperature conditions (16°C, 26°C, or 36°C) differed from one another. To facilitate intuitive interpretation of the data distribution and pressure change patterns, two types of visualization were used.

First, heatmaps were generated to display the mean contact pressure at each combination of temperature and anatomical site for each manufacturer, allowing visual comparison of overall pressure levels and trends. Second, box plots were created by pooling all anatomical sites within each temperature condition to illustrate the median, interquartile range, and variability of the pressure distributions.

All statistical analyses were conducted using the Statsmodels and SciPy libraries in Python, and the level of statistical significance was set at 0.05 [19,20].

RESULTS

1. CT image analysis results

The acquired CT images were imported into the Eclipse™ treatment planning system (Varian Medical Systems, USA), and the outer margin of each thermoplastic mask was delineated by applying a consistent Hounsfield unit (HU) threshold across all conditions. To ensure reproducible structure extraction, a threshold of −600 HU and a smooth level of 0 were used for all reconstructions. Repeated structure generation under the same settings confirmed that inter-scan differences in calculated mask volume were not statistically significant, indicating good consistency of the segmentation procedure.

Table 1. Dice similarity coefficients of thermoplastic head-and-neck masks according to cooling temperature and elapsed time after molding.

Manufacturer	Time elapsed	16°C	26°C	36°C
A	7 days	0.827	0.781	0.704
	30 days	0.827	0.790	0.645
B	7 days	0.848	0.814	0.801
	30 days	0.782	0.769	0.769

For each experimental condition, the CT-derived geometry of the thermoplastic mask was compared with the mask geometry at the time of initial fabrication, and the resulting DICE values were calculated. The DICE values obtained under each temperature and time condition are summarized in Table 1.

When the masks were fabricated at 16°C, both materials (manufacturers A and B) showed the highest DICE values, indicating minimal geometric shrinkage and relatively high structural stability. In contrast, as the fabrication temperature increased, the DICE values gradually decreased, with the lowest values observed at 36°C. This trend suggests that molding at higher temperatures leaves the thermoplastic material in a more unstable molecular configuration, so that residual stress remains after cooling and leads to increased shrinkage and shape deformation over time.

For manufacturer A, the DICE value at 7 days after fabrication was 0.827 under the 16°C condition, corresponding to roughly a 17% deviation from perfect overlap, whereas at 36°C the DICE value decreased to 0.704, corresponding to about a 30% deviation. Similarly, for manufacturer B, the DICE value at 16°C was 0.848 (approximately 15% deviation), while at 36°C it declined to 0.801 (approximately 20% deviation), confirming the same tendency of greater geometric change at higher fabrication temperatures.

These findings indicate that higher fabrication temperatures are associated with an increased shrinkage tendency of the thermoplastic material. In addition, when comparing the geometry immediately after fabrication with that at 30 days, a slight overall reduction in DICE values was observed across conditions, reflecting gradual structural relaxation and subtle time-dependent shrinkage of the material. This decrease in DICE was more pronounced for masks molded at higher temperatures than for those fabricated

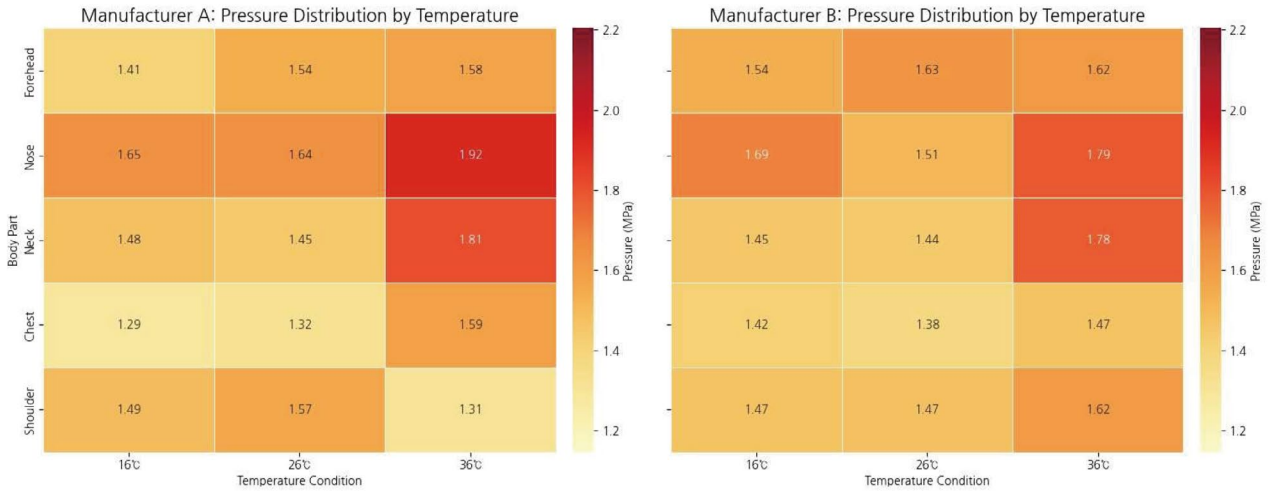

Fig. 7. Heatmaps of mean contact pressure (MPa) by manufacturer, cooling temperature, and anatomical site for thermoplastic head-and-neck masks.

at lower temperatures, confirming that the initial molding temperature has a substantial impact on subsequent geometric stability. Overall, thermoplastic masks fabricated and cooled from higher residual temperatures exhibited greater shrinkage and poorer shape reproducibility than those produced under lower-temperature conditions.

2. Pressure measurement in pressure-sensitive film

For each type of thermoplastic mask, contact pressure was measured at five anatomical sites—forehead, nasal bridge, neck, chest, and shoulder—under three cooling conditions (16°C, 26°C, and 36°C) using pressure-sensitive film. From the developed films, the red (R) channel values were extracted, and changes were compared across three time points: immediately after fabrication (1st measurement), 7 days after fabrication (2nd measurement), and 30 days after fabrication (3rd measurement). The R value was defined as the median intensity of the red channel within the selected region on the film, and the mean of the values obtained at each site was used for analysis. Because the film darkens as pressure increases, the R value is inversely related to contact pressure; that is, lower R values correspond to higher applied pressure.

Fig. 7 shows heatmaps of the mean contact pressure for thermoplastic head-and-neck masks from manufacturers A and B, according to cooling temperature (16°C, 26°C, and 36°C) and anatomical site. Overall, masks from manufacturer A exhibited relatively small and uniform changes in pressure across different temperature conditions. In contrast, masks from manufacturer B showed a pronounced increase in pressure at specific sites as the cooling temperature increased, indicating a greater temperature dependence of contact pressure for this material.

For manufacturer A, the pressure distributions at 16°C and 26°C were almost identical across all anatomical sites. Even at 36°C, only a modest overall increase in pressure was observed. The forehead and nasal bridge consistently showed the highest pressure levels at all temperatures; however, the absolute differences in pressure between temperature conditions remained limited. In contrast, the shoulder region showed a slight decrease in mean pressure at 36°C compared with the lower-temperature conditions.

For manufacturer B, the effect of temperature was much more pronounced. At 36°C, the pressure at the nasal bridge and neck increased markedly and these two sites exhibited the highest pressures among all measurements. In particular, the nasal bridge showed a steep rise in pressure at 36°C compared with 16°C. The forehead and shoulder also demonstrated increased pressure at 36°C, although the magnitude of these changes was smaller than that observed at the nasal bridge and neck.

Fig. 8 compares the distribution of contact pressure (MPa) across all anatomical measurement sites for thermoplastic masks from manufacturers A and B under each cooling

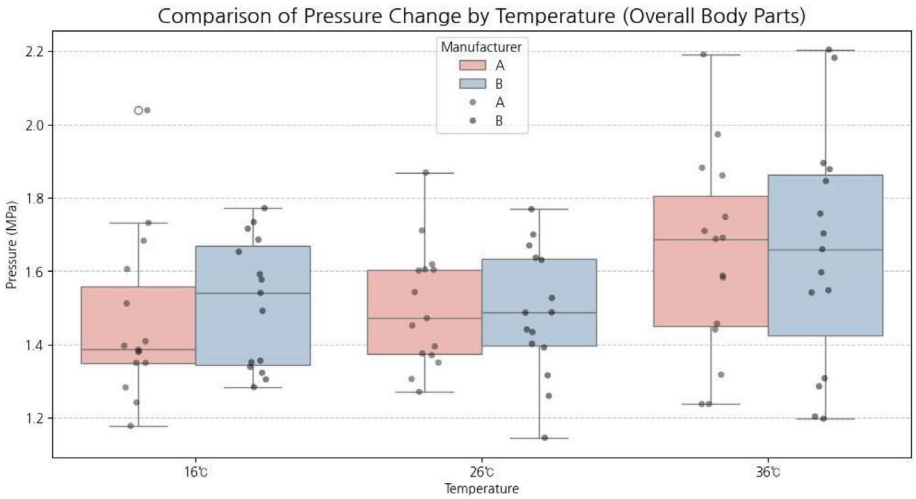

Fig. 8. Box plots of overall contact pressure (MPa) distributions by manufacturer and cooling temperature, integrating all anatomical measurement sites.

temperature condition (16°C, 26°C, and 36°C). At 16°C, the median pressure was approximately 1.39 MPa for manufacturer A and 1.45 MPa for manufacturer B. At 26°C, the median pressures were about 1.48 MPa for manufacturer A and 1.49 MPa for manufacturer B, indicating very similar central tendencies between the two manufacturers. At 36°C, the median pressure increased to approximately 1.70 MPa for manufacturer A and 1.67 MPa for manufacturer B, demonstrating an overall upward shift in pressure compared with the lower-temperature conditions.

When comparing the spread of the distributions (box height and interquartile range), both manufacturers showed comparable variability at 16°C and 26°C. However, at 36°C, the width of the box for manufacturer B increased markedly compared with that for manufacturer A, indicating greater variability in pressure measurements under the high-temperature condition. This pattern is consistent with the results of the two-way analysis of variance. After controlling for the effect of anatomical site, temperature had a statistically significant impact on pressure for masks from manufacturer B ($p=0.0483$), whereas no statistically significant temperature effect was observed for masks from manufacturer A ($p=0.1155$).

DISCUSSION

This study quantitatively evaluated the influence of residual temperature during fabrication of thermoplastic head-and-neck immobilization masks on both geometric stability and the contact pressure transmitted to the patient. The findings indicate that control of the cooling phase—particularly the residual temperature of the mask immediately after molding—is directly linked to mask quality and patient experience in clinical practice.

CT-based analysis using the DICE values clearly demonstrated that higher residual temperatures at the time of fabrication were associated with reduced geometric stability. For both manufacturers A and B, masks cooled to 16°C maintained the highest shape similarity over time, whereas those cooled at 36°C exhibited the lowest DICE values. These observations are consistent with previous reports on thermoplastic materials, which have shown that inadequate cooling from a high-temperature state prevents full relaxation of the polymer molecular network and leads to greater accumulation of residual stress during the cooling process [8]. Karimiani further reported that non-uniform or insufficient cooling can induce volumetric shrinkage and temperature gradients, generating significant thermal residual stresses that may manifest as additional shrinkage or shape deformation over time [21,22].

The localized pressure increases observed in this study, particularly at the nasal bridge and neck, have significant clinical implications for patient experience. The nasal bridge is a bony prominence with thin overlying soft tissue, making it highly susceptible to pressure-related pain when

subjected to the elevated contact pressures observed under high-temperature molding conditions. Furthermore, excessive pressure on the neck region is critically relevant to patient compliance, as it is directly linked to the sensation of choking. This physical discomfort can trigger claustrophobia and anxiety, potentially leading to involuntary patient movement during treatment. Therefore, minimizing pressure peaks at these specific anatomical sites through adequate cooling is essential not only for geometric precision but also for reducing treatment-limiting distress.

Based on these findings, the reduced shape reproducibility (i.e., lower DICE values) observed under the 36°C condition can be interpreted as a consequence of the mask solidifying before it has sufficiently cooled. In this situation, the internal structure of the thermoplastic material cannot fully stabilize, and greater residual stress remains within the mask. Over time, this residual stress is released in the form of additional shrinkage and geometric distortion. Such thermo-mechanical behavior can ultimately reduce setup reproducibility in radiotherapy by increasing patient posture changes and positioning errors, underscoring the clinical need to standardize and strictly control the cooling process.

In addition, DICE values showed a slight decrease between 7 and 30 days for all manufacturers and all temperature conditions. This time-dependent reduction was most pronounced for masks fabricated at 36°C, indicating that high-temperature molded masks do not achieve complete structural stabilization even after the initial cooling phase, and continue to undergo subtle deformation over time.

The pressure-sensitive film analysis further revealed clear manufacturer-dependent differences in the thermal stability of the masks, which are directly relevant to the level of contact pressure actually experienced by patients during radiotherapy. For masks from manufacturer A, the magnitude of pressure change across the three temperature conditions (16°C, 26°C, and 36°C) was small, and the overall distribution remained relatively uniform. Consistent with this, statistical analysis ($p = 0.1155$) showed no significant effect of temperature on contact pressure. These results suggest that the material used by manufacturer A is less sensitive to temperature variations and is capable of maintaining structural stability and a uniform pressure profile across a range of molding conditions.

In contrast, masks from manufacturer B showed a marked increase in pressure at the nasal bridge and neck under the high-temperature (36°C) molding condition, accompanied by a clear widening of the pressure distribution. Consistently, the two-way ANOVA indicated that temperature had a statistically significant effect on pressure for manufacturer B ($p = 0.0483$), suggesting that this material is highly sensitive to residual heat. When molded at higher temperatures, it appears more prone to pronounced thermal shrinkage and the generation of non-uniform, localized pressure peaks at specific anatomical sites.

These manufacturer-dependent differences highlight the critical impact of cooling temperature during thermoplastic mask fabrication on both geometric stability and pressure uniformity. In this study, DICE analysis showed that the highest shape stability was consistently achieved under the lowest residual temperature (16°C), whereas higher-temperature conditions led to greater geometric deviation over time. This pattern is in line with previous reports on the cooling behavior of thermoplastic materials. Kamal and Karimiani have described how insufficient cooling prevents full stabilization of the internal polymer network, resulting in higher residual stress accumulation and promoting progressive shrinkage and shape distortion as time elapses [21,22]. More recently, Miron et al. also reported that, for both thermoplastic and three-dimensional (3D) printed fixation masks, securing adequate thermal stability immediately after fabrication is crucial, and inadequate cooling can lead to structural deformation and reduced immobilization accuracy [23].

Taken together, these findings indicate that fabrication protocols for thermoplastic masks should include a standardized cooling procedure that sufficiently lowers the residual temperature after molding in order to minimize long-term shrinkage and preserve setup reproducibility over the course of repeated treatments. Furthermore, because the temperature sensitivity of mask materials can differ substantially between manufacturers, thermal stability should be considered alongside immobilization strength when selecting a head-and-neck mask system. Localized pressure increases associated with high-temperature molding may exacerbate patient discomfort, claustrophobia, and intrafraction motion; thus, careful control of cooling temperature represents a practical strategy to improve both patient experience and treatment precision.

Finally, the use of a single standardized phantom to isolate temperature effects limits the assessment of anatomical diversity, such as variations in neck circumference or BMI.

Therefore, future studies utilizing phantoms representing diverse morphotypes are recommended to validate these findings across broader patient populations.

CONCLUSION

This study evaluated the impact of residual temperature immediately after molding on the geometric stability and contact pressure distribution of thermoplastic head-and-neck immobilization masks.

DICE analysis showed that, for both manufacturers, masks molded at 36°C had the lowest geometric stability, whereas those molded at 16°C were the most stable. This finding implies that high-temperature molding leads to increased residual stress within the material, which can manifest as greater long-term shrinkage and deformation.

Pressure analysis revealed clear differences between manufacturers. For manufacturer A, the pressure distribution changed very little across temperature conditions, and the effect of temperature was not statistically significant ($p=0.1155$). In contrast, masks from manufacturer B showed higher pressure and greater variability at 36°C, particularly at specific anatomical sites, and the temperature effect was statistically significant ($p=0.0483$).

Overall, these results indicate that appropriate control of the cooling process is critical for ensuring both geometric stability and minimizing patient-perceived pressure. In particular, the 16°C cooling condition provided the most favorable combination of structural stability and uniform pressure distribution, supporting the need for standardized cooling protocols in clinical practice.

ACKNOWLEDGMENTS

The authors would like to thank the staff of the Department of Radiation Oncology at Keimyung University Dongsan Hospital for their valuable support and assistance with this study.

REFERENCES

1. Delishaj A, Ursino S, Pasqualetti F, Cristaudo A, Vidiri A, Bruni A, et al. Set-up errors in head and neck cancer treated with IMRT: a systematic review and recommendations for PTV margins. Radiat Oncol. 2018;13:163. https://doi.org/10.3857/roj.2017.00493
2. Thornton AF Jr, Sandler HM, Ten Haken RK, McShan DL, Fraass BA. A head immobilization system for radiation simulation, CT, and daily treatment using Aquaplast thermoplastic masks. Int J Radiat Oncol Biol Phys. 1991;21:1325-30. https://doi.org/10.1016/0958-3947(91)90045-4
3. Boda-Heggemann J, Walter C, Rahn A, Wertz H, Lohr F, Wenz F, et al. Repositioning accuracy of two different mask systems-3D analysis. Radiother Oncol. 2006;80:333-9. https://doi.org/10.1016/j.ijrobp.2006.08.054
4. Gilbeau L, Octave-Prignot M, Loncol T, Renard L, Scalliet P, Gregoire V, et al. Comparison of setup accuracy of three different immobilization systems for head and neck radiotherapy. Radiother Oncol. 2001;58:185-93. https://doi.org/10.1016/s0167-8140(00)00280-2
5. Lastrucci A, Al-Saffar M, Leech M, Short M, Beadle BM, Lee C, et al. Open-face masks in radiotherapy: a scoping review of use, patient comfort and immobilisation accuracy. Cancers (Basel). 2024;16:2899. https://doi.org/10.3390/cancers16162899
6. Yoram F, Dharsee N, Mkoka DA, Maunda K, Kisukari JD. Radiation therapists' perceptions of thermoplastic mask use for head and neck cancer patients undergoing radiotherapy at Ocean Road Cancer Institute in Tanzania: a qualitative study. PLoS One. 2023;18:e0282160. https://doi.org/10.1371/journal.pone.0282160
7. Nixon JL, Cartmill B, Turner J, Pigott AE, Brown E, Wall LR, et al. Exploring the prevalence and experience of mask anxiety for the person with head and neck cancer undergoing radiotherapy. J Med Radiat Sci. 2018;65:282-90. https://doi.org/10.1002/jmrs.308
8. Dovell V, Bennett J, Fish J, Frantzis J, Lawford C, Rogers P. Assessment of comfort and shrinkage in four styles of thermoplastic masks. J Med Imaging Radiat Sci. 2014;45:247-53. https://doi.org/10.1016/j.jmir.2014.03.028
9. Lundin E, Nyholm T, Dufva S, Bergström P, Pettersson N. Open or closed: experience of head and neck radiotherapy masks—patient preferences for open or closed masks and whether an open mask can reduce discomfort and anxiety. J Med Radiat Sci. 2025;72:74-84. https://doi.org/10.1002/jmrs.825
10. Kim SY, Park JW, Park J, Yea JW, Oh SA. Fabrication of 3D printed head phantom using plaster mixed with polylactic acid powder for patient-specific QA in intensity-modulated radiotherapy. Sci Rep. 2022;12:17500. https://doi.org/10.1038/s41598-022-22520-6
11. Jäkel O, Ackermann B, Ecker S, Ellerbrock M, Heeg P, Henkner K, et al. A novel phantom setup for commissioning of

scanned ion beam therapy. Radiat Oncol. 2019;14:67. https://doi.org/10.1186/s13014-019-1281-5
12. Lee N, Chuang C, Quivey JM, Phillips TL, Akazawa P, Weinberg V, et al. Skin toxicity due to intensity-modulated radiotherapy for head-and-neck cancer: dosimetric correlations and dose-volume relationships. Int J Radiat Oncol Biol Phys. 2002;53:630-7. https://doi.org/10.1016/S0360-3016(02)02756-6
13. Lu Y, Song J, Yao X, An M, Shi Q, Huang X. 3D printing polymer-based bolus used for radiotherapy. Front Oncol. 2021;11:669456. https://doi.org/10.18063/ijb.v7i4.414
14. Shin YS, Byun SJ, Kim B, Kim M. Assessing the reliability of 3D-printed custom silicone boluses in radiotherapy: thickness and air bubble considerations. Appl Sci. 2025;15:10486. https://doi.org/10.3390/app151910486
15. Pang G, Lu Y, Xu Y, Meng Q, Song J. The investigation of opening modes of head and neck thermoplastic mask for radiotherapy based on finite element analysis. Radiat Oncol. 2025;20:64. https://doi.org/10.1186/s13014-025-02648-1. PMID: 40301880; PMCID: PMC12038929
16. Saha A, Harowicz MR, Mazurowski MA. A machine learning approach to automatic segmentation of head and neck organs at risk in CT images using the Dice similarity coefficient as performance metric. Med Phys. 2023;50:e1-12.
17. Bachus KN, DeMarco AL, Judd KT, Horwitz DS, Brodke DS. Measuring contact area, force and pressure for bioengineering applications: using Fuji Film and TekScan systems. Med Eng Phys. 2006;28:483-8. https://doi.org/10.1016/j.medengphy.2005.07.022
18. Patterson R, Pogue D, Viegas S. The effects oftimeand lightexposure on contactand pressure measurements using Fuji prescale film. Iowa Orthop J. 1997;211:63-6.
19. Virtanen P, Gommers R, Oliphant TE, Haberland M, Reddy T, Cournapeau D, et al. SciPy 1.0: fundamental algorithms for scientific computing in Python. Nat Methods. 2020;17:261-72. https://doi.org/10.1038/s41592-019-0686-2
20. Seabold S, Perktold J. Statsmodels: Econometric and statistical modeling with Python. Proc 9th Python in Science Conf (SciPy 2010). 2010:57-61.
21. Kamal MR, Lai-Fook RA, Hernandez-Aguilar JR. Residual thermal stresses in injection moldings of thermoplastics: a theoretical and experimental study. Polymer Eng Sci. 2002; 42:1098-114. https://doi.org/10.1002/pen.11015
22. Karimiani HG. Analysis of residual stresses in thermoplastic composites using cooling shrinkage models [master's thesis]. Montreal (QC): Concordia University; 2015.
23. Miron VM, Etzelstorfer T, Kleiser R, Raffelsberger T, Major Z, Geinitz H. Evaluation of novel 3D-printed and conventional thermoplastic stereotactic high-precision patient fixation masks for radiotherapy. Strahlenther Onkol. 2022;198:1032-41. https://doi.org/10.1007/s00066-022-01963-w